

Pair Dispersion in Turbulence: The Subdominant Role of Scaling

Mark Peter Rast

*Laboratory for Atmospheric and Space Physics, Department of Astrophysical and Planetary Sciences,
University of Colorado, Boulder, Colorado 80309, USA*

Jean-François Pinton

*Laboratoire de Physique, Ecole Normale Supérieure de Lyon, CNRS UMR5672, Université de Lyon,
46 allée d'Italie, F-69364 Lyon, France*

(Received 15 July 2011; published 14 November 2011)

The mixing properties of turbulent flows are, at first order, related to the dynamics of separation of particle pairs. Scaling laws for the evolution in time of the mean distance between particle pairs $\langle r^2 \rangle(t)$ have been proposed since the pioneering work of Richardson. We analyze a model which shares some features with 3D experimental and numerical turbulence, and suggest that pure scaling laws are only subdominant. The dynamics is dominated by a very wide distribution of “delay times” t_d , the duration for which particle pairs remain together before their separation increases significantly. The delay time distribution is exponential for small separations and evolves towards a flat distribution at large separations. The observed $\langle r^2 \rangle(t)$ behavior is best understood as an average over separations that individually follow the Richardson-Obukhov scaling, $r^2 \propto t^3$, but each only after a fluctuating time delay t_d , where t_d is distributed uniformly.

DOI: 10.1103/PhysRevLett.107.214501

PACS numbers: 47.27.-i, 47.32.-y

Scalar transport by turbulent flows is naturally described in terms of Lagrangian particle dispersion. This most generally requires knowledge of the statistics of n -particle dynamics $\{\mathbf{r}_1(t), \mathbf{r}_2(t), \dots, \mathbf{r}_n(t)\}$ which in turn hinges on a closure scheme [1]. Recent theoretical and phenomenological efforts have focused on the dynamics of tetrads [2,3] as tracers of nonlinear (triadic) interactions. A simpler first step is the pair dispersion problem, acquiring an understanding of the evolution in time of the distance between two Lagrangian fluid particles $\langle r^2(t) \rangle_{\text{pairs}}$. Recent reviews [4,5] have concluded that for such 2-point statistics the predictions of the celebrated Kolmogorov 1941 theory are not as readily observed as for 1-point statistics. We examine the issue here using a stochastically driven point-vortex model [6]. The model creates a 2D flow via the interaction of randomly generated vortices of random amplitude. Generation followed by the merger of vortices mimics some ingredients of three-dimensional vortex stretching and dissipation.

Let us first recall some fundamental features of the 2-point dispersion problem and associated scaling hypotheses in the context of the Kolmogorov phenomenology of turbulence. In the limit of very short times, comparable to the dissipative time scale τ_η , neighboring fluid particles are expected to separate exponentially following the largest Lyapunov exponent of the local (smooth) flow. On the other hand, for very long times, comparable to the flow integral correlation time T_L , turbulence is expected to be diffusive and so one expects $\langle r^2 \rangle_{\text{pairs}} \propto t$. Modeling efforts have thus concentrated on the intermediate range of time scales, $\tau_\eta \ll t \ll T_L$ (the “inertial” subrange). In this range, there is no characteristic time or length scale and

the constraint of a fixed mean energy transfer rate $\langle \epsilon \rangle$ suggests the relationship known as the Richardson-Obukhov law [7,8], $\langle r^2 \rangle = g \langle \epsilon \rangle t^3$, where g is a dimensionless constant. (Note: this scaling also results if the particles execute a random walk in velocity space, i.e., if one assumes a diffusive behavior for the velocity difference between two points, $(\delta u(t))^2 \propto t$, then $r(t) = \int \delta u(t') dt' \sim t^{3/2}$. There is some suggestion that single point Lagrangian trajectories effectively sample velocity space in this way—Eq. 18 in [6].)

However, the inertial range is limited in its extent, $T_L/\tau_\eta \sim \text{Re}^{1/2}$ with Re the flow Reynolds number, and it has been argued that one should include the initial separation r_0 in the above dimensional argument since the relative dynamics of a particle pair introduces an origin of time, that at which their locations coincide. Taking t_0 as the time over which the initial separation is important, one looks for a scaling solution $\langle r^2 \rangle_{\text{pairs}} = r_0^2 f(t/t_0)$. Batchelor [9] suggested that the characteristic time t_0 for the initial entrainment of the particle pair by an eddy of size r_0 follows the Richardson-Obukhov law, $t_0 \sim \langle \epsilon \rangle^{-1/3} r_0^{2/3}$, and thus for times less than t_0 pair separation evolves as $\langle r^2 \rangle = g' (\langle \epsilon \rangle r_0)^{2/3} t^2$, with g' another dimensionless constant related to the Kolmogorov constant for the longitudinal second-order velocity structure function, $g' = (11/3)C_2$. For $t_0 \ll t \ll T_L$, the Richardson-Obukhov law still holds.

Such scaling behaviors have been difficult to identify in experiments, observations, or direct numerical simulations. It has been suggested that it is because of the limited inertial range accessible to numerical studies that they only hint at possible asymptotic Richardson-Obukhov

behavior [10], though exit-time statistics seem to provide clearer evidence [11,12]. On the other hand, experimental studies point to Batchelor scaling when the behavior of $\langle r^2(t) \rangle$ is directly investigated [13,14] or to a Richardson-Obukhov regime if time and space are suitably rescaled to account for the initial phase (r_0, t_0) [15]. Here we suggest an alternative, that while the Richardson-Obukhov scaling may underlie the dynamical behavior of individual particle pairs it does so only intermittently, interrupted by “trapping delays” with a broad distribution of durations, and it is the averaging over these delays which dominates the observed $\langle r^2 \rangle$ behavior [16].

We employ a simplified point-vortex flow model, the main characteristics of which [6] are only briefly recalled here. Point vortices are randomly generated at a constant average rate with Gaussianly distributed intensity in a two-dimensional periodic domain of dimension x_{\max}^2 . The velocity field is built from the contributions of each individual vortex as

$$\mathbf{u}(\mathbf{x}) = \sum_{k=1}^N \frac{\Gamma_k}{2\pi|\mathbf{x} - \mathbf{x}_k|} [\hat{\mathbf{z}} \times (\mathbf{x} - \mathbf{x}_k)], \quad (1)$$

where Γ_k are the circulations, and the range of contribution is truncated at the distance x_{\max} . Vortex merger is imposed when vortices are closer than a fixed critical separation, unit one distance. (We note, that for simplicity of notation (as compared to [6]) we scale the distance between Lagrangian particles here so that $r = 2\pi\sqrt{x^2 + y^2}$.) The system would ultimately decay due to the merger of oppositely signed vortices except for the continuous stirring by the aforementioned generation of new point vortices at random locations in the domain. Effective stretching occurs when such vortices are generated within the merging distance of an existing like-sign vortex. The velocity field created in this way shows surprisingly strong similarities to 3D turbulence. For example, the agreement between the Lagrangian intermittency (1-point statistics) in the model and that found experimentally is quite remarkable [6]. We will show here (Fig. 2) that this is true for pair dispersion (2-point statistics) as well.

The point-vortex model solutions discussed in this Letter each continue, with the same parameter values, from the endpoint of the simulation presented in [6]. They were seeded with a grid of $N \in [2304, 2304, 2304, 1024]$ Lagrangian particle pairs, randomly oriented and with initial separations between pair members of $r_0 \in [0.05, 0.2, 0.5, 1.0]$, respectively. The positions and velocities of each particle were tracked as the flow evolved. Examples of particle trajectories and corresponding pair separations $r(t)$ are shown in Fig. 1, with thin and bold lines marking individual pair member paths and an open circle marking their initial positions. It is clear even from this limited sample of trajectories that individual pairs show distinctive behaviors. Pair separation initiates after differing initial delays and can be intermittent even at late times,

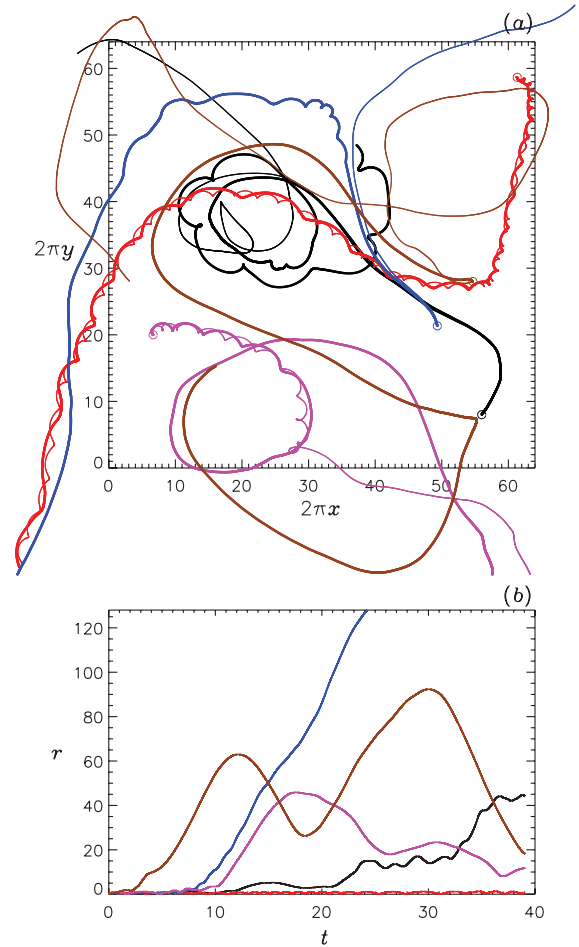


FIG. 1 (color). (a) Example trajectories of particle pair members. Trajectories of individual members of each pair are shown with thin and bold lines. (b) Corresponding (by color) time traces of their separation $r(t)$. All pairs were initiated, at sites indicated by open circles, with initial separation $r_0 = 0.2$.

stalling due to trapping events. These differences occur even when the pairs share the same initial separation, as they do in Fig. 1.

The solid curves in Fig. 2 show the time evolution of the mean squared separation of the particle pairs, and are qualitatively similar to those of dispersion in both laboratory (e.g., [13,15]) and three-dimensional numerical experiments (e.g., [12,17]): (1) the pair separation grows steeply after an initial phase during which the particles remain in close proximity (though this phase is exaggerated by the logarithmic scale) and (2) no clear scaling behavior emerges. The slopes of the curves observed in previous studies differ, ranging from values of 2 in [13] to 3 in [12,15], and 4.5 (possibly 4) in [17]. In our work, the curves collapse when time is shifted so that the origins of time in the $r_0 > 0.05$ cases align with the times required to reach $\langle r^2 \rangle = r_0^2$ in the $r_0 = 0.05$ case (black, blue, and red dashed curves in Fig. 2) and show a slope of about 4 over a limited range.

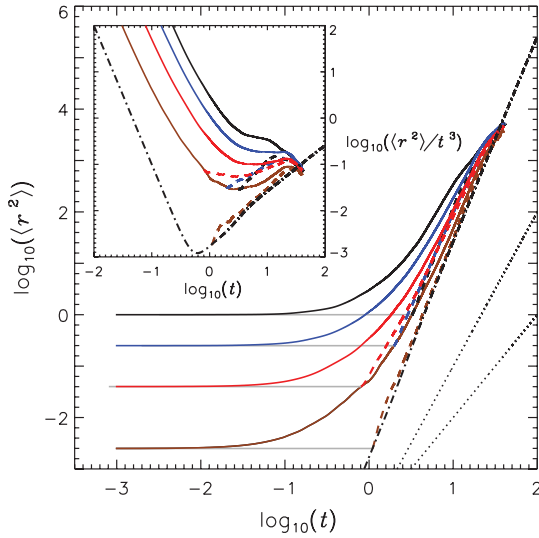


FIG. 2 (color). Pair dispersion $\langle r^2(t) \rangle$ for initial separations $r_0 = 1.0, 0.5, 0.2$, and 0.05 shown with black, blue, red, and brown curves, respectively. Inset shows t^3 compensated curves. Dashed black, blue, and red plot dispersion with shift in time based on time to reach $\langle r \rangle = r_0 = 1.0, 0.5$, and 0.2 in $r_0 = 0.05$ solution. Dash-dotted curves show results of the uniform waiting time distribution model (see text), and the brown dashed curve the $r_0 = 0.05$ solution with time shifted to account for time to reach $\langle r_0 \rangle = 0.5$ in that. Fiducial $\langle r^2(t) \rangle \propto t^2$ and $\langle r^2(t) \rangle \propto t^3$ dotted lines are shown for reference.

The scaling discrepancies seen in previous studies have usually been taken to reflect the initial conditions of the pair measurements, and several approaches have been proposed to account for them. Perhaps the most convincing evidence for scaling comes from the exit-time analysis proposed in [11,12], but even in that analysis the scaling range is quite limited. Critically, such exit-time analysis relies on the assumption that the time t_0 required to reach a separation significantly larger than the initial r_0 has a distribution peaked around the dimensional value $(r_0^2 / \langle \epsilon \rangle)^{1/3}$. We show here that this is not the case—at least not in this simplified model of a turbulent flow. As seen in Fig. 3, the distribution of such times is very broad. It is exponential with a time scale of order of the flow integral time for small initial separations, but rapidly evolves towards a flat distribution as r_0 grows into the inertial range. We will return in detail to these properties, which are the main findings of our study, but we first demonstrate that such a broad distribution of delay times has an order-one effect on the dynamics of separation.

A crude model of the dynamics underlying each individual pair separation can be constructed as a combination of successive delays and separations, as in [16]. Here we consider only two such steps: in the first, the particles remain at their original separation distance r_0 for a time t_d , a time chosen from a uniform distribution, as suggested by the data. In the second, they separate according to an algebraic law, $r^2 = r_0^2 + (t - t_d)^\alpha$, where α is a constant

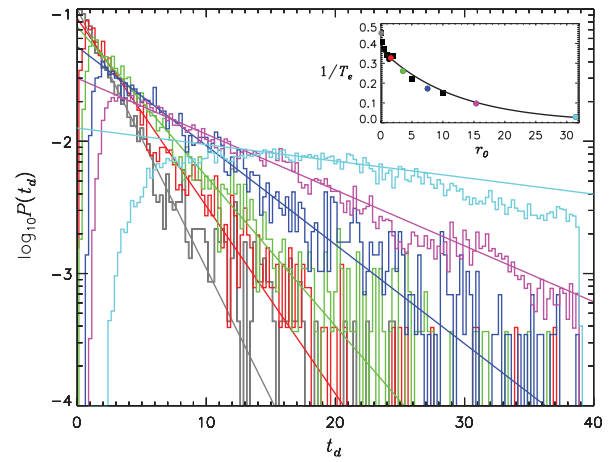


FIG. 3 (color). Probability density of delay times, time to double the initial separation, for narrow ranges of r_0 (one unit wide) characterized by mean $r_0 = 0.05, 1.29, 3.57, 7.53, 15.4$, and 31.4 (gray, red, green, blue, fuchsia, and cyan respectively). Solid lines plot exponential fits to distribution tails. Values of these are plotted in the inset as function of r_0 , along with the same measure from a range of simulations (black symbols).

which may be set to 3 for an expected Richardson scaling or 2 for Batchelor-like behavior. The result of averaging over this simplified dynamics is shown in Fig. 2 as the black dash-dotted curve. Two features are readily apparent: (i) the model behavior is in very good agreement with the with numerical data of the simulation, (ii) a scaling plateau $\langle r^2 \rangle / t^3 \sim C$ is not observed, even when a perfect Richardson scaling is imposed in the model—in fact an underlying Batchelor scaling (i.e., t^2) in the separation phase actually yields a better Richardson $\langle r^2 \rangle / t^3$ plateau. This is because a random sequence of algebraic separations with uniformly distributed delays would actually lead to the average pair separation growing as $\int (t - t_d)^\alpha dt \propto t^{\alpha+1}$ [18]. An underlying Richardson t^3 scaling leads to the t^4 behavior observed in Fig. 2, when the delay time distribution is uniform. Other broad delay time distributions, non-uniform, produce somewhat different slopes, all between 3 and 4. We conclude that similarly the actual dynamics of separation is dominated by the wide distribution of delay times. Additional evidence for this is found in the observed behavior of the $r_0 = 0.05$ solution. When time in that solution is shifted to account for the time needed to reach the $r_0 = 0.05$ initial condition, and when that temporal offset is based on the uniform waiting time distribution model, it follows the black dash-dotted curve of the model very closely (as shown by the dashed brown curve in Fig. 2). In other words, pair dispersion in the point-vortex model behaves as the superposition of Richardson-Obukov trajectories with onset times sampling a uniform distribution of delays.

We thus now aim to quantify the delay times t_d observed in the point-vortex simulations. We define the delay time as the time needed for the distance between a particle pair to

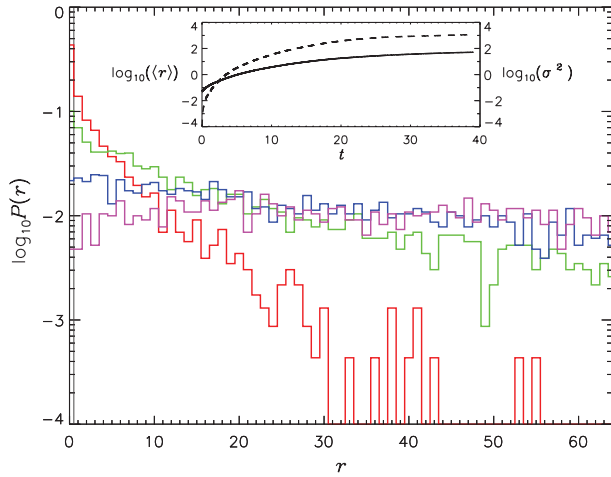


FIG. 4 (color). Probability density of pair separations r in $r_0 = 0.05$ solution as a function of time $t = 0, 10, 20, 30,$ and 40 (gray, red, green, blue, and fuchsia, respectively). Inset plots logarithm of the mean (solid line) and variance (dashed line) of distribution as a function of time. Note that the variance rapidly exceeds the mean by an order of magnitude.

grow by a factor of 2, and note that the change in terminology from exit time, used by previous authors, to delay time here is nontrivial. We imagine the delay time to occur not strictly at the beginning of the measurement, to account for effects of the initial condition, but continuously throughout the time series as subsequent trapping events at large scales occur with finite probability.

To illustrate the delay time probability distribution we analyze the evolution of pairs with narrowly specified values of initial separation r_0 , while understanding that at any time t a range of effective “initial” separations is sampled by the solution involving many pairs (Fig. 4). The delay time distributions as a function of r_0 are shown in Fig. 3. Very wide distributions occur for all values of r_0 , with the distribution widening with increased r_0 . That is, even if many pairs separate right away, a significant fraction can remain bound for times comparable to the large scale eddy turnover time. The distribution $P(t_d)$ has a marked peak only for quite small r_0 values and becomes flat as r_0 grows into the inertial range. From the exponential behavior of the distribution, one may extract a characteristic time T_e of the “bound phase” of the pair dynamics. It grows with the initial separation r_0 as shown in the inset of Fig. 3; the functional form of this growth is also exponential with a characteristic scale of about 1/5th of the flow domain.

In Fig. 4 we turn to the evolution of the distribution of pair separations with time in the point-vortex flow (starting from the smallest initial separation $r_0 = 0.05$ studied). The distribution quickly broadens, possibly to a stretched exponential at early times, as previously reported in 2D [19] and 3D [15] experiments, numerical studies [10,16], and some statistical models [20,21]. At later times, $P(r)$ flattens. The inset of Fig. 4 displays the evolution of the variance of $P(r)$ compared to its mean, and shows that the

variance in pair spacing exceeds the mean value after very short times. The system rapidly evolves to a state in which the mean is a poor representation of the pair separation statistics. Moreover, the wide distribution of pair separations observed is associated with a wide distribution of delay times (Fig. 3), and these dominate further evolution of $\langle r^2 \rangle$ as we have illustrated by the highly simplified uniform delay time distribution model. While careful data analysis may extract behavior tangent to scaling regimes [12,15], fixed time $\langle r^2 \rangle(t)$ or fixed scale $\langle t \rangle(r^2)$ statistics are fundamentally subdominant. This finding explains the elusive evidence for scaling in previous work: successive trappings by coherent structures generate a very wide distribution of delay times which dominate the functional form of the average separation rate. Scaling is not prevented by a lack of inertial range dynamics, but is instead blurred by intermittent dynamics which generate the wide distribution of delay times.

The authors thank A. Pouquet and acknowledge support from ENS de Lyon, ANR-07-BLAN-0155, and the National Science Foundation through the National Center for Atmospheric Research and Award No. 0457552. M. P. R. thanks P. Garaud for the warm hospitality provided during ISIMA2010 at the University of California, Santa Cruz.

-
- [1] S. B. Pope, *Turbulent Flows* (Cambridge University Press, Cambridge, 2005).
 - [2] A. Pumir, B. I. Shraiman, and M. Chertkov, *Phys. Rev. Lett.* **85**, 5324 (2000).
 - [3] L. Chevillard and C. Meneveau, *Phys. Rev. Lett.* **97**, 174501 (2006); L. Biferale *et al.*, *Phys. Rev. Lett.* **98**, 214501 (2007).
 - [4] B. L. Sawford, *Annu. Rev. Fluid Mech.* **33**, 289 (2001).
 - [5] J. P. L. C. Salazar and L. R. Collins, *Annu. Rev. Fluid Mech.* **41**, 405 (2009).
 - [6] M. P. Rast and J.-F. Pinton, *Phys. Rev. E* **79**, 046314 (2009).
 - [7] L. F. Richardson, *Proc. R. Soc. A* **110**, 709 (1926).
 - [8] A. M. Obukhov, *Izvestiia Akademii nauk SSSR Ser. Geogr. Geofiz.* **5**, 453 (1941).
 - [9] G. K. Batchelor, *Q. J. R. Meteorol. Soc.* **76**, 133 (1950).
 - [10] B. L. Sawford, P. K. Yeung and J. F. Hackl, *Phys. Fluids* **20**, 065111 (2008)
 - [11] V. G. Artale *et al.*, *Phys. Fluids* **9**, 3162 (1997).
 - [12] L. Biferale *et al.*, *Phys. Fluids* **17**, 115101 (2005).
 - [13] M. Bourgoin *et al.*, *Science* **311**, 835 (2006).
 - [14] N. T. Ouellette *et al.*, *New J. Phys.* **8**, 109 (2006).
 - [15] J. Berg *et al.*, *Phys. Rev. E* **74**, 016304 (2006).
 - [16] S. Goto and J. C. Vassilicos, *New J. Phys.* **6**, 65 (2004).
 - [17] D. R. Osborne *et al.*, *Phys. Rev. E* **74**, 036309 (2006).
 - [18] The authors thank Douglas Gough for pointing this out.
 - [19] M.-C. Jullien, J. Paret, and P. Tabeling, *Phys. Rev. Lett.* **82**, 2872 (1999).
 - [20] F. Nicolleau and J. C. Vassilicos, *Phys. Rev. Lett.* **90**, 024503 (2003).
 - [21] G. Pagnini, *J. Fluid Mech.* **616**, 357 (2008).